FLIGHT RESULTS AND LESSONS LEARNED FROM THE ØRSTED ATTITUDE CONTROL SYSTEM

T. Bak, M. Blanke, R. Wisniewski

Institute of Electronic Systems, Aalborg University
DK-9220 Aalborg Ø, Denmark
E-mail: {tb,blanke,raf}@control.auc.dk

ABSTRACT

Small satellites provide a growing possibility for carrying out space experiments within an affordable budget. Keeping cost down requires a design philosophy, which involves some degree of risk. Sharing the understanding and experience gained from flight operation is important for evaluating the design and provide valuable input to future projects of similar nature.

The small satellite Ørsted was launched on 23 February 1999. Besides demonstrating new technical capabilities based on new hardware and inexpensive actuators, Ørsted provides flight experience with on-board autonomy. The attitude control and estimation algorithms are integrated with a supervisory control architecture that enables reconfiguration in real time, based on mission phase and contingency requirements. This paper discusses and evaluates the Ørsted attitude control system operations history.

1. INTRODUCTION

Few if any small satellite missions to date have been able to demonstrate the ability to perform high profile science missions. One of the main obstacles is the lack of proper attitude determination and control needed to facilitate mainstream scientific missions. Small satellites also involves some degree of risk to keep down cost. Experience from flight is therefore an important tool in evaluating the design philosophy.

This paper discusses the results from the first six months of operation of the Ørsted spacecraft. The focus is on the ACS(Attitude Control Subsystem) operations history.

1.1. The Ørsted Satellite

Ørsted was launched on 23 February 1999. The satellite carries a science payload used to study the Earth's magnetic field, distribution in the solar wind, and temperature/humidity profiles in the atmosphere. The satellite is three axis stabilized using a three sets of perpendicular electromagnetic torquer coils consisting of six physical coils.

The attitude control and estimation algorithms are integrated into a supervisory control architecture that enables reconfiguration in real time, based on mission phase and contingency operation requirements. This provides some level of fault tolerance with graceful degradation in case of severe faults.

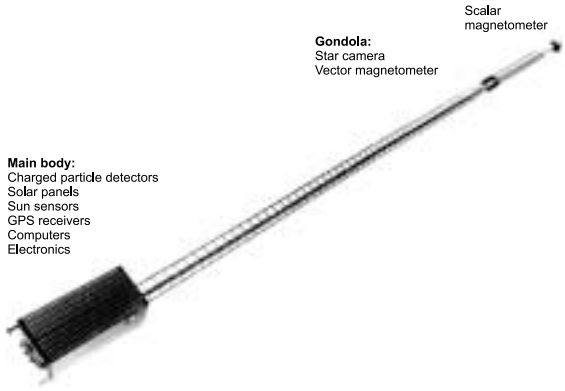

Figure 1: The Ørsted satellite. The main body is $600 \times 450 \times 300$ mm and the total weight is 62 kg.

The Ørsted budget for development and operation was 120 million Danish Kroner or equivalently 18 million USD. The fundamental operational parameters are summarized in Table 1.

Table 1: *Operational parameters of the Ørsted satellite.*

Orbit	Inclination	96.62 deg.
	Ascending node	14:39 Local time
	Height	600-850 km
Attitude	Stabilization	Active three-axis and gravity gradient stabilized
	Control	Magnetic
Mass	Total	62 kg
	Payload	13 kg (including booms and antennas)
Telemetry	Ground stations	Copenhagen and Aalborg, Denmark
	Transmitter	S-band transmitter (2.2 GHz) and receiver (2.0 GHz)
	Downlink rate	4 or 256 kbits/sec
Power	Nominal Power	31 W (GaAs solar panels)
Computer	Main computer	Two 80C186/16 Mhz CPUs
	Storage	16 Mbyte, 13 hours of science
	Software	Ada developed based on formal methods

The ACS algorithms are implemented in the general command and data handling of the satellite. A science package consisting of a star camera and a magnetometer are

mounted on a eight meter long instrument boom. The boom is deployed after an initial detumbling phase and the three-axis attitude is maintained with the boom zenith pointing.

The main control requirements driving the design were

- *Detumbling.* Damping of kinetic energy. The satellite should be aligned with the local magnetic field with $-z$-axis (bottom) along field lines for deployment over Denmark.
- *Three-axis stabilization.* After boom deployment the reference attitude is zenith pointing. The angular deviation from vertical should be maintained within a $\pm$10 deg. (1 sigma). The yaw reference is changing, but the reference tracking should be within $\pm$ 20 deg. (1 sigma). The angular velocity is required below 10 deg./minute at all time.
- *Contingencies.* A number of contingency situation should be handled autonomously.

A philosophy for the development of fault-tolerant control has been adopted in the design of the ACS [1]. Attitude determination and control algorithms are reconfigurable in real time. This makes it possible to accommodate changed mission phases, faults, and contingencies. An on-board supervisor [2] monitors the spacecraft status and reconfigures ACS algorithms accordingly, to optimize the performance of the system. All on-board autonomous transitions can be controlled through uplinked, time-tagged telecommands. Further operational flexibility is provided by allowing adjustments of all on board ACS parameters while the ACS is running. The main ACS architecture is outlined in Figure 2.

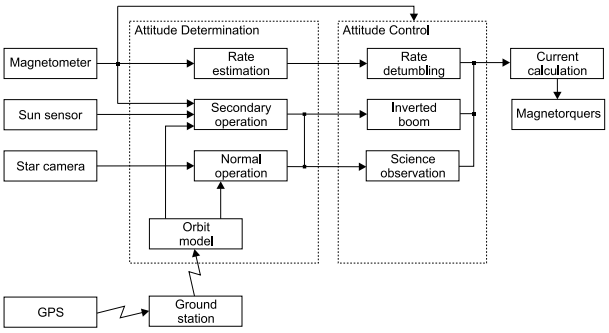

Figure 2: The attitude control system architecture.

On top of the fundamental control system layer, fault detection algorithms and supervisor logic, oversees the ACS performance and manages state changes, autonomously.

2. ATTITUDE CONTROL

The interaction between the Earth's magnetic field and the magnetic moment generated by magnetorquer coils produces a torque used for the attitude corrections. The control action is inherently nonlinear and difficult to use since the control torque can only be generated perpendicular to the geomagnetic field vector. This has been a serious obstacle for using magnetic control for three-axis attitude control so far, and to the best of our knowledge, Ørsted is the first three axis stabilized spacecraft using solely magnetic coils for attitude control.

Dependent on the mission phase three separate attitude controllers have been developed: the rate detumbling controller, the science observation controller and the inverted boom controller. The first two have successfully tested in space and are described in the next subsections. The Ørsted's instrument boom has never been pointing towards the Earth, therefore the third one, the contingency operation controller, has never been activated in space. The details of the inverted boom controller can be found in [3].

2.1. Rate Detumbling Control

The objective of the rate detumbling controller is to generate a magnetic moment, such that the kinetic energy of the satellite is dissipated and it is turned in the direction of the local geomagnetic field vector. The influence of the gravity gradient on the satellite in a boom stowed configuration is negligible.

The kinetic energy, E_{k}, of the rotary motion is:

$$E_{\mathrm{k}} = \frac{1}{2}\boldsymbol{\Omega}_{\mathrm{pi}}^T \, \mathbf{I} \, \boldsymbol{\Omega}_{\mathrm{pi}}, \tag{1}$$

where $\boldsymbol{\Omega}_{\mathrm{pi}}$ is the satellite angular velocity with respect to an inertial coordinate system, $\mathbf{I}$ is the inertia tensor.

Lyapunov theory has been applied in [4] to prove that E_k is dissipated if the following control law is implemented:

$$\mathbf{m} = -k \, \dot{\mathbf{B}}, \tag{2}$$

where $\mathbf{m}$ is the magnetic moment, $\mathbf{B}$ is the local geomagnetic field vector, and k is a positive constant (control gain).

This controller does not ensure directional control, however. To establish radio contact with the ground station in Denmark and make boom deployment possible , the rate detumbling controller is altered such that the z-axis (in boom direction) of the satellite tracks the inverse direction of the geomagnetic field. This is achieved by adding a constant term to the control law in Eq. (2):

$$\mathbf{m} = -k \, \dot{\mathbf{B}} - \mathbf{m}_{\mathrm{const}}, \tag{3}$$

where $\mathbf{m}_{const} = [0 \; 0 \; -m_{\mathrm{const}}]^T, \; m_{\mathrm{const}} > 0$. Now the satellite acts like a compass needle which tends to align with the negative direction of the local geomagnetic field, while adequate angular velocity damping is retained.

Remark 1 *The controller in Eq. (3) does not use any a priori knowledge of the moments of inertia nor the information of the placement of the magnetometer, since the only feedback information used is the rate of changes of the geomagnetic field vector.*

Remark 2 *In the rate detumbling phase the magnetometer is placed in the spacecraft main body, therefore the control duty cycle is divided into two periods: the measure period with* $\mathbf{m} = \mathbf{0}$*, and the control period with the magnetic moment generated according to Eq. (3).*

Remark 3 *It is possible to modify all parameters of the rate detumbling controller in the ACS on-board software: the filter constants for computing* $\dot{\mathbf{B}}$*, the controller gain* k *and the bias magnetic moment* $\mathbf{m}_{const}$*.*

2.2. Rate Detumbling Results in Space

The rate detumbling controller was first initiated for 20 minutes in order to check performance of the Ørsted ACS. After this check the ACS was activated with the initial parameter set. The tracking of the geomagnetic field was achieved within 40 deg accuracy. over the North and South Poles. The ACS team concluded that the satellite had a small residual magnetic moment, which could be overcome by sending a larger bias m_{const}, which was increased from 3 to 12 Am^2. This modification resulted in tracking within desired 5 degrees. The Ørsted team was ready for boom deployment.

Due to boom safety reasons it was decided that the boom should be deployed over Southern Africa. This imposed an additional task on the ACS not considered before the launch. The satellite had to establish a radio contact with the ground station in Denmark by tracking the negative direction of the geomagnetic field vector, but deployment had to be done over Southern Africa, i.e. the satellite should track the positive magnetic field vector. A time-tagged command was send to change the sign of m_{const} over the equator passes. Due to flexibility of the ACS software this task was fulfilled with success and the Ørsted boom was deployed.

The time history of the angle between the geomagnetic field vector and the boom direction is depicted in Figure 3. The satellite initially tracked the negative B-field vector, then the reference was change to track the positive B-field vector and the boom deployment started. The 8 meter long boom was deployed during 10 minutes. During this operation the satellite rate reduced dramatically due to increase of the moments of inertia. It is seen in Figure **??** that already after 3 minutes the satellite started to librate regularly.

2.3. Science Observation Control

The objective of the science observation controller is to three-axis stabilize the satellite. The details of the control

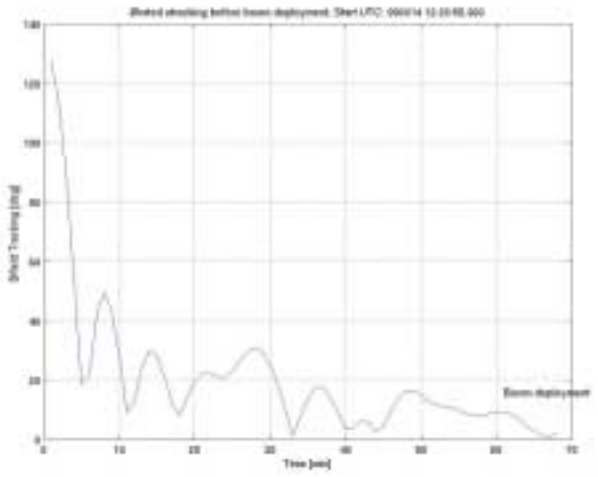

Figure 3: The satellite initially tracks the inverse geomagnetic field, then changes to tract the positive B-field vector and the boom deployment starts..

synthesis is addressed in [4] and [3].

The controller takes the following form

$$\boldsymbol{m}(t) = (\mathbf{H}\,\boldsymbol{\Omega}_{\mathrm{po}}(t)) \times \boldsymbol{B}(t), \tag{4}$$

where $\boldsymbol{\Omega}_{\mathrm{po}}$ is the angular velocity of the spacecraft in the Local Vertical Local Horizontal (LVLH) coordinate system [1] and $\mathbf{H}$ is a positive-definite constant matrix.

There are two main reasons to suggest this feedback:

1. It contributes to dissipation of kinetic energy.
2. It provides four stable equilibria: the axis of the minimal moment of inertia points in the direction of the zenith, and the axis of the largest moment of inertia is parallel to the normal to the orbital plane:

$$\{(\boldsymbol{\Omega}_{\mathrm{po}}, \boldsymbol{k}_{\mathrm{o}}, \boldsymbol{j}_{\mathrm{o}}) : (\mathbf{0}, \pm\boldsymbol{k}, \pm\boldsymbol{j})\}, \tag{5}$$

where $\boldsymbol{k} := \begin{bmatrix}0 & 0 & 1\end{bmatrix}^{\mathrm{T}}, \boldsymbol{j} := \begin{bmatrix}0 & 1 & 0\end{bmatrix}^{\mathrm{T}}$.

Remark 4 *Magnetic torquing following Eq. (4) obviously introduces time dependency in the equations of the satellite motion. This time variation is periodic by nature, which*

arises from two superimposed periodic changes of the local geomagnetic field vector. One is due to revolution of the satellite about the Earth with the period corresponding to the orbital period, the second due to rotation of the Earth. The orientation of the orbit is fixed in an inertial coordinate system, thus the rotation of the Earth is visible

[1] The z axis, local vertical, points towards the center of the Earth. The y axis points in the direction of the negative angular momentum. The x axis, local horizontal, completes the coordinate system

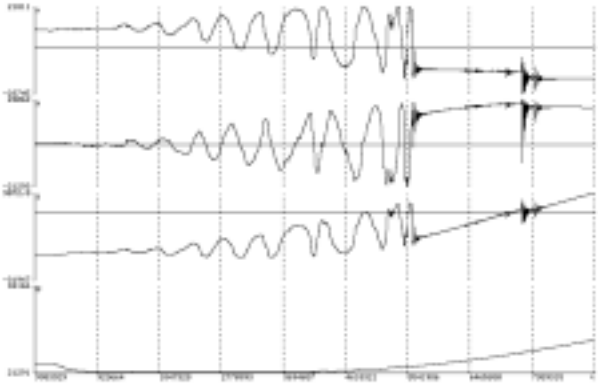

Figure 4: The 8 meter long boom is deployed during 10 minutes. Already after 3 minutes the satellite starts to librate regularly.

as variation of the geomagnetic field vector's y component with frequency $1/24$ *hours. Summarizing the spacecraft with the control law (4) is governed by periodic differential equation. The Krasovskii-LaSalle lemma in [5] is applied in the proof of asymptotic stability of the control law (4). The Lyapunov candidate function is the sum of kinetic energy of rotary motion, potential energy generated by the gravity gradient and the energy originating from the revolution of the satellite around the Earth.*

The controller (4) is used for the rate control in the case of contingency, when the satellite is spinning about the boom axis - the axis of the minimum moment of inertia. It is also used for three axis stabilization in the neighborhood of two references: $\{(\boldsymbol{\Omega}_{\rm po}, \boldsymbol{k}_{\rm o}, \boldsymbol{j}_{\rm o}) : (\mathbf{0}, \boldsymbol{k}, \pm\boldsymbol{j})\}$.

Remark 5 *The assumption of exact knowledge of the principal moments of inertia was not made in the proof of asymptotic stability of the control law (4). Thereby the controller is robust towards modeling uncertainties.*

In order to incorporate different references and better disturbance attenuation additional attitude feedback was incorporated

$$\boldsymbol{m}(t) = (\mathbf{H}\boldsymbol{\Omega}_{\rm pr}(t)) \times \boldsymbol{B}(t) - (\epsilon\mathbf{q}(t)) \times \boldsymbol{B}(t), \quad (6)$$

where $\boldsymbol{\Omega}_{\rm pr}$ is the angular velocity of the satellite with respect to the Reference Coordinate System (RCS). The RCS is defined relative to the LVLH by the rotation about the z-axis of an angle θ - the yaw reference. $\mathbf{q}$ is the vector part of ${}^{\rm p}_{\rm r}\mathbf{q}$, i.e. the quaternion, representing the transformation from the RCS to the spacecraft fixed coordinates. $\mathbf{H}$ and ϵ are the coefficient matrices.

Remark 6 *The gain matrices* $\mathbf{H}$ *and* ϵ *are calculated using Floquet theory, [6], and plotting the locus of the the characteristic multipliers of the closed loop system, [7].*

Remark 7 *All control parameters* $\mathbf{H}$, ϵ, θ, *and* $\omega_{\rm o}$ *are modifiable. To reach extra flexibility in the controller structure a modifiable saturation limit on the magnetic moment and the bias magnetic moment were implemented.*

Remark 8 *The yaw corrections are primarily carried out in the equatorial regions, whereas the yaw controllability is completely lost over the poles.*

2.4. Experience in Space of Science Observation Control

After boom deployment the science observation controller was activated. The attitude information was accessible from the star camera and the magnetometer based extended Kalman filter. For the three-axis attitude control the star camera was used, the extended Kalman filter was implemented for the contingency operation.

The star camera has several limits discussed in Section 4: the Sun and the Earth exclusion angles and maximum rate limit. The first stage after the boom deployment was to despin the satellite below the star camera rate limit. The control law (4) was used together with the extended Kalman filter. The three-axis attitude control was the next stage. Shortly after the controller (6) was initiated the ACS team understood that the exclusion angles and the orientation of the sun as observed from the orbit left the ACS with the attitude margin below the limit specified in the requirements. As time passed and the orbit precessed this margin was increased to an acceptable level. The next problem to be faced was to understand and find a solution to a negative coupling between the star camera and the ACS. The lack of availability of the signal from the star camera produced discrepancy between the reference attitude and the actual satellite orientation. In the periods when the star camera data were available the controller tried to correct the attitude, but the generated control signal excited the resonance modes, despite slow body rate below 10 deg./min. This phenomenon was later explained by the fact that the boom eigenfrequencies were 5 times lower than predicted by the manufacturer. The resonance of the boom resulted in dropouts of the star camera and lack of the attitude input to the attitude controller. This scenario was repeated several times until the satellite started to spin and the controller (4) had to be activated again. The solution to this problem was

1. To increase the validity flag in the star camera software. This resulted in a greater number of valid attitude data.

2. To decrease the rate gain $\mathbf{H}$ in the control law (6). This resulted in slower satellite motion.

3. To reduce the generated magnetic moment to 1.5 Am^2. This resulted in the reduction of the pick current in the magnetorquer coils.

The outcome of the implementation of these three remedy actions was closing of the Ørsted satellite commissioning phase in September 1999. The performance of the three-axis attitude controller is illustrated in Figure 5. The attitude converges to the reference: pitch and roll to 0 deg., yaw to -90 deg.

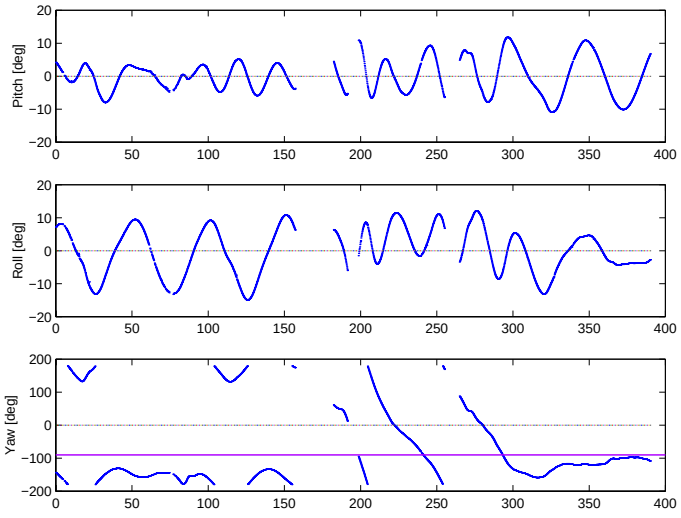

Figure 5: The attitude converges to the reference: pitch and roll to 0 deg., yaw to -90 deg..

3. AUTONOMY

No serious faults have been detected during the first six months of Ørsted operation. To give a simple example of the autonomous operation of the ACS, we consider in this paper only the period right after launch. Shortly after the start of detumbling algorithm, coil driver faults were detected in all three sets of coils. As the coupling between coil current and magnetometer measurements is well known, the magnetometer measurements is one of the information sources for the coil driver fault detection. The influence of the coil currents on the magnetometer measurements is shown in Figure 6.

At t_0 the coils are commanded to zero, to allow measurement of the background field, 100 msec. later the coil currents are set again, and at $t_0 + t_m$ msec. the magnetometer is read and compared with the computed disturbance. Due to an problem with the coil driver the measurements deviate from the expected and a fault is detected. During detumbling all six coils are used the ACS supervisor hence disable coil output and declare the coil driver as faulty. The problem is clearly that the coil driver output is twice the demanded for about 100 msec. The problem was solved raising the t_m parameter in the fault detection module. This prevented the fault from surfacing on board, and allowed for active detumbling. The coil error had no significant influence on the remaining part of the detumbling after the detection problem was solved. During science observation the control cycle runs at a 10 sec. interval and the effect may be ignored. Analysis of results from environmental test performed prior to launch indicates that the problem with the coil drivers was present prior to launch.

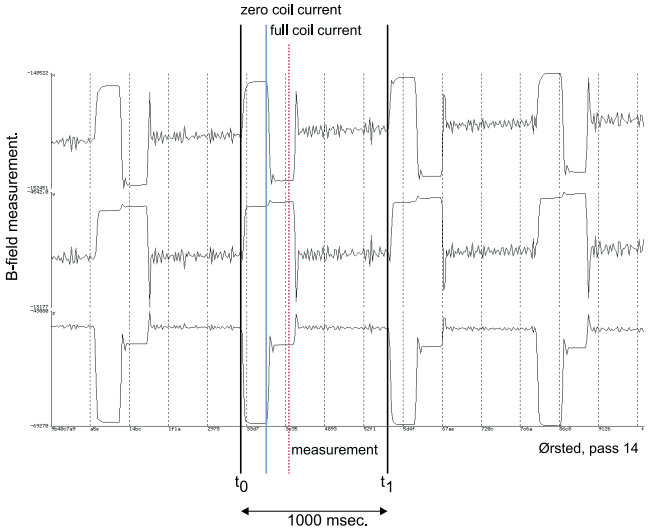

Figure 6: Magnetometer measurements, detumbling.

4. ATTITUDE DETERMINATION

During science observation the primary instrument for attitude information is the star camera (see [8]). Both the ACS and the star camera are at their limit of operation, and the interaction between the camera and the control system has proved problematic. Most star camera dropouts are caused by one of these two phenomena

- *Rapid angular motion.* Caused by boom vibrations induced by thermal effects on the boom or ACS control action.
- *Blinding.* The star camera exclusion angles are violated.

The influence on the ACS due to lack of star camera attitude is investigated in the following. An example of a loss of star camera data is depicted in Figure 7.

The star camera attitude drops out at approximately 6 min. which cause the rate estimate to diverge from zero, and the coil currents therefore increase in order to compensate. In this case the coil current stays below 100 mA (5% of allowable current), and yaw angle remains within the requirements. The rate estimate is based on simple filtering of the star camera attitude and the inversion of kinematics As no attitude updates are available the filter is allowed to diverge from the true rate. At approximately 10 minutes the dropout occurs again, and the control system output is autonomously temporarily disabled for approximately 15 min..

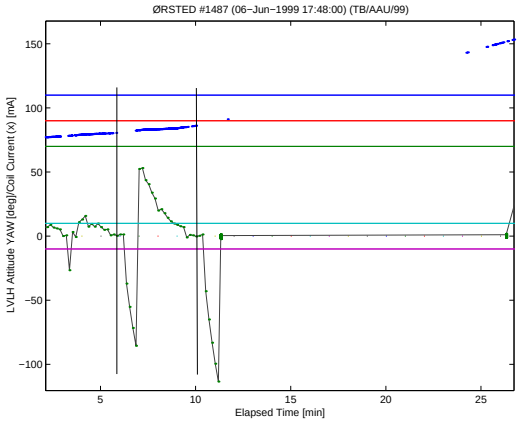

Figure 7: Yaw attitude and coil currents (dotted line).

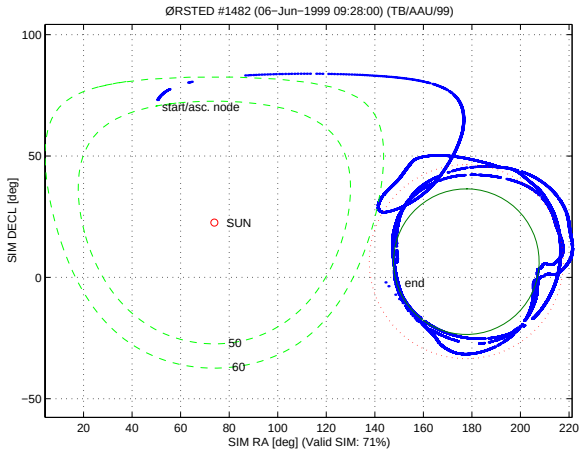

Figure 8: World plot of attitude.

The initial rate filter was tuned to track a fast attitude motion and hence diverged quickly in case of camera dropouts. In numerous situations this lead to coil currents that caused a yaw spin. At spin rates above 10 deg./min a magnetometer based attitude and rate estimate was utilized to bring the satellite back within the star camera operational constraints.

High sensitivity of the star camera caused frequent drop outs, which in turn lead to undesirable control action and more camera dropouts. This loop was finally broken, by reducing the star camera sensitivity combined with modifications of ACS parameters. A reduction in the controller gains and modification of the rate filter, has effectively removed the problems outlined above.

The dynamic interaction between ACS and star camera was never tested prior to launch in order to save on integration time and cost. The flexibility of the ACS and the camera has been vital for the in-flight commissioning of the two systems.

4.1. Star Camera Blinding

The other source of star camera dropouts is violation of the exclusion angles. An example is shown in Figure 8.

The small circle at the right of Figure 8 represents perfect attitude tracking, whereas the dark line represents the actual attitude over a number of orbits. The dotted circle represent the 1 sigma boundaries on the attitude requirements. The curves at the right are the angular distances to the sun. The star camera exclusion angles varies between 40 and 60 deg. It is thus clear from Figure 8, that the angular separation between camera boresight and nominal attitude is minimal, and the camera will experience blinding, even with the ACS within specifications. As the mission progresses the angular separation becomes larger as the orbit plane moves towards local noon.

4.2. Secondary Operation

When the star camera constraints are violated, attitude and rates are estimated based on the magnetometer measurements. The three components of the magnetic field are fused with time updated predictions in a Kalman filter. A typical situation, where the attitude control maintains a near -90 deg. attitude is given in Figure 9.

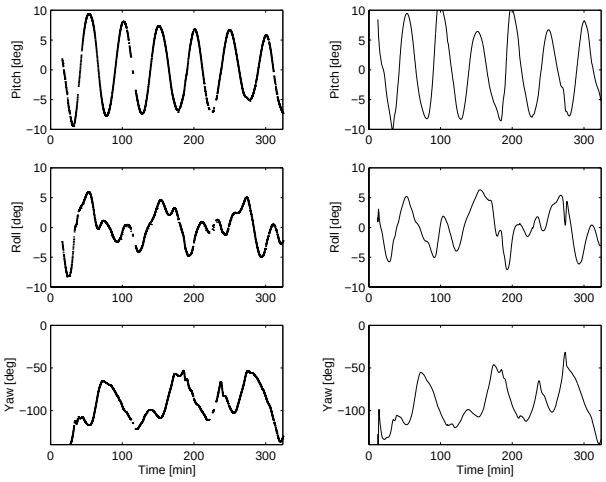

Figure 9: Ørsted results from orbits 2539-2542 (August 18 1999 UTC: 19:07:56). Pitch/roll/yaw estimates from the star camera (left) and from the magnetometer (right).

5. CONCLUSIONS - AFTER END OF COMMISSIONING

The development of the Ørsted small satellite program was a fast development, spiral like approach. The main focus was on the most critical issues, requirements to formal documentation were much reduced compared with

space industry practice, the requirements to fast turn-around time during development were fairly high. Communication channels were kept minimal, daily teleconferences replaced monthly progress reports. Despite experiments in project management, requirements to functionality and performance of the final product were similar to those of much larger projects.

In general, this approach has been an asset for the Ørsted satellite. The budget was kept comparatively low, the development was completed without significant delays, and the overall functionality and operation of the satellite is very satisfactory indeed.

The lessons learnt are classical, but we dare anyway to propose slight modifications to the small satellite development paradigm that would enhance the final, quality of the product, in particular remove system faults, which could have been avoided with a fairly small additional effort while the spacecraft was at ground. The vehicle to reach such improvement would be better integration and integration testing. This point was given a lower priority towards the end of the development and end funding. The result has been a somewhat longer commissioning phase in space than foreseen. The cost and complexity of commissioning in space could be estimated to a factor of 10 times larger compared to similar tests before launch. Since some tests are very difficult to perform at ground, a trade-off need to be made between time spent on ground tests and commissioning in space, however.

5.1. Difficulties that took time to overcome

In the Ørsted case, the commissioning phase was about four times longer than expected. The primary reasons were

- An initial defect in boom orientation (the 45 deg. twist) after deployment made the sun blinding of the star camera a regular event.
- Boom flexibility is experienced with more than five times lower first torsional eigenmode than predicted by the manufacturer, and thermal ”quakes” passing the eclipse boundaries gives rise to vibration that smears the star camera image and it stops delivering attitude measurements. This happens frequently, and is not a rare, irregular event as expected. A not tested interaction phenomena between star camera pause and attitude control could accelerate the yaw motion to further prolong the periods where angular velocity was too large for the star camera.
- The fall-back estimation of attitude was made difficult due to integer implementation of an extended Kalman filter. Coping with large turn rates as needed had a penalty in very low level quantization effects in the filter. The filter gave very good rate estimates that were used many times to recover the spacecraft, but low rate accuracy was not good enough as to allow operation without the star camera.
- Timing errors (time jump every 2.5 days is present in the ACS and a similar defect is present in the satellite on-board HW.
- Synchronization between the instruments have been a major obstacle for scientific accuracy of data. While not affecting the ACS, commissioning time is longer, the more simultaneous problems one has.
- Finally, ground communication difficulties caused several command loss events to be diagnosed by the satellite, leading to undesired close-down of the space segment. Parallel commissioning of the ground stations, control center, and the basic on-board service systems is proved time consuming.

5.2. Features that contributed to overall success

The main features of the attitude control system included a flexible structure and access to essentially all internal variables and parameters through dedicated debugging commands. The main contributing factors were:

- Considering the complexity of the Ørsted satellite, system faults have been few and have all been accommodated
- Effective diagnosis, debugging and parameter modify commands were implemented in a very limited code size and proved a crucial feature. Other systems required time-consuming patches where the ACS system accepted modify-commands to perform similar actions.
- The versatility of the ACS system made it possible to make not foreseen control and a not foreseen recovery (rate control) mode
- A fully three-axis magnetic control concept was developed and proven to function in space. Ørsted is, to our knowledge, the first fully three axis stabilized in space using solely magnetorquers for control.
- Satellite detumbling was successfully completed and faster than anticipated.
- The orientation of the satellite before boom deployment was replanned after launch and successfully completed.
- Operation in normal mode suffers from the star camera-ACS interaction, which led to gain reduction and lower pointing accuracy, however, the success of the scientific mission is not pointing accuracy but low angular velocity and high observation availability.
- Relative high autonomy – no ground station interaction with the control system, except for reference

changes and an orbit parameter upload every 7 days.

The progress of the commissioning is illustrated in Figure 10 where star camera availability were increased for 40 to about 95 percent in three steps. The large jumps in performance occurred when the real reasons to difficulties were resolved and subsequent star camera patches and ACS parameter adjustments were made.

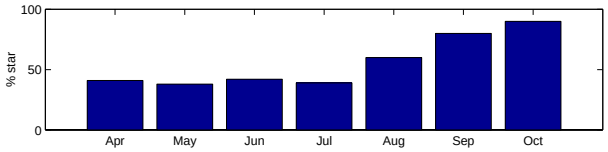

Figure 10: Star camera availability during commissioning.

5.3. Recommendations

The lessons learned could be summarized to three main issues. First, the science team should be very active during the early design phase, making explicit requirements to the platform performance. The rapid progress and short development cycle of a small satellite makes no time/money available for re-iterations. Second an increased focus on integration and complete system performance assessment can cut precious time from commissioning in space. Third, the transient non-foreseen conditions should be better supported by the ACS functionality to make accommodation easier.

In conclusions, Ørsted is now producing data of science quality in about 90% of time. With a small satellite project and daytime-manned operator station, the autonomous features of the satellite have proved their value and the mission of Ørsted is considered a solid success.

REFERENCES

1. Blanke M Sep. 1995, Aims and tools in the evolution of fault-tolerant control, in *ESF COSY Workshop, Rome*.

2. Bøgh S A & al Oct. 1995, Onboard supervisor for the ørsted satellite attitude control system, in *5th ESA workshop on Artificial Inteligence and Knowledge Based Systems for Space*.

3. Wisniewski R & M Blanke 1999, Three-axis attitude control based on magnetic torquing, *Automatica*, 7(35), 1201–1214.

4. Wisniewski R Dec. 1996, *Satellite Attitude Control Using Only Electromagnetic Actuation*, Ph.D. thesis, Aalborg University.

5. Vidyasagar M 1993, *Nonlinear Systems Analysis*, Prentice Hall.

6. Mohler R 1991, *Nonlinear Systems*, vol. Dynamics and Control, Prentice Hall.

7. Wisniewski R Aug. 1997, Linear time varying approach to satellite attitude control using only electromagnetic actuation, in *AIAA Guidance, Navigation, and Control Conference, New Orleans,*.

8. Bak T Nov. 1996, Onboard attitude determination for a small satellite, in *Proceedings Third International Conference on Spacecraft Guidance, Navigation and Control Systems*. ESA.